mRNA vaccination compared to infection elicits an IgG-predominant response with greater SARS-CoV-2 specificity and similar decrease in variant spike recognition

Katharina Röltgen[1]†, Sandra C. A. Nielsen[1]†, Prabhu S. Arunachalam[2], Fan Yang[1], Ramona A. Hoh[1], Oliver F. Wirz[1], Alexandra S. Lee[3], Fei Gao[2], Vamsee Mallajosyula[2], Chunfeng Li[2], Emily Haraguchi[1], Massa J. Shoura[1], James L. Wilbur[4], Jacob N. Wohlstadter[4], Mark M. Davis[2,5,6], Benjamin A. Pinsky[1,7], George B. Sigal[4], Bali Pulendran[1,2,5], Kari C. Nadeau[3,8]‡, Scott D. Boyd[1,3]‡*

[1]Department of Pathology, Stanford University School of Medicine, Stanford, CA, USA.

[2]Institute for Immunity, Transplantation and Infection, Stanford University, Stanford, CA, USA.

[3]Sean N. Parker Center for Allergy & Asthma Research, Stanford, CA, USA.

[4]Meso Scale Diagnostics LLC, Rockville, Maryland, USA.

[5]Department of Microbiology and Immunology, Stanford University, Stanford, CA, USA.

[6]Howard Hughes Medical Institute, Stanford University, Stanford, CA, USA.

[7]Department of Medicine, Division of Infectious Diseases and Geographic Medicine, Stanford University, Stanford, CA USA

[8]Department of Medicine, Division of Pulmonary, Allergy & Critical Care Medicine, Stanford University, Stanford, CA, USA.

*Corresponding author: sboyd1@stanford.edu

†these authors contributed equally to this work.

‡ these authors contributed equally to this work.

Abstract

During the severe acute respiratory syndrome coronavirus 2 (SARS-CoV-2) pandemic, new vaccine strategies including lipid nanoparticle delivery of antigen encoding RNA have been deployed globally. The BioNTech/Pfizer mRNA vaccine BNT162b2 encoding SARS-CoV-2 spike protein shows 95% efficacy in preventing disease, but it is unclear how the antibody responses to vaccination differ from those generated by infection. Here we compare the magnitude and breadth of antibodies targeting SARS-CoV-2, SARS-CoV-2 variants of concern, and endemic coronaviruses, in vaccinees and infected patients. We find that vaccination differs from infection in the dominance of IgG over IgM and IgA responses, with IgG reaching levels similar to those of severely ill COVID-19 patients and shows decreased breadth of the antibody response targeting endemic coronaviruses. Viral variants of concern from B.1.1.7 to P.1 to B.1.351 form a remarkably consistent hierarchy of progressively decreasing antibody recognition by both vaccinees and infected patients exposed to Wuhan-Hu-1 antigens.

Keywords

COVID-19, BioNTech/Pfizer BNT162b2, mRNA vaccine, serology, electrochemiluminescence, SARS-CoV-2, variants of concern, endemic coronaviruses, antibodies

Introduction

In 2020, following decades of research to develop messenger RNA (mRNA) vaccines, and accelerated by the urgent need for countermeasures against the coronavirus disease 2019 (COVID-19) pandemic, the U.S. FDA authorized two mRNA vaccines, BNT162b2 (BioNTech/Pfizer) and

mRNA-1273 (Moderna/NIAID). mRNA vaccines are a promising alternative to conventional vaccine approaches in part because a relatively consistent biomolecule can be used to generate a variety of antigens in the vaccine recipient (Pardi et al., 2018a). They have been shown to stimulate protective immune responses to viral infections in pre-clinical models (Pardi et al., 2017, 2019; Richner et al., 2017; Vogel et al., 2021), and recently have demonstrated high efficacy and safety in clinical trials for COVID-19 prevention (Baden et al., 2021; Polack et al., 2020; Walsh et al., 2020). mRNA vaccines mimic some aspects of viral infection by using the host cell's translational machinery to transiently express properly folded vaccine antigens *in situ,* driving strong humoral and T cell responses (Sahin et al., 2014; Zhang et al., 2019). It remains to be determined precisely how the immune system responds to RNA vaccines and their other components such as lipid nanoparticles, compared to other vaccine platforms or infection.

Immune correlates of protection from COVID-19 have not been fully elucidated, but both humoral and cellular responses may contribute to preventing and containing infection (McMahan et al., 2021; Ni et al., 2020; Rydyznski Moderbacher et al., 2020). Most neutralizing antibodies target the receptor-binding domain (RBD) of SARS-CoV-2 spike (S) and prevent binding to the host angiotensin-converting enzyme 2 (ACE2) receptor (Yuan et al., 2021). The BNT162b2 mRNA vaccine (as well as mRNA-1273) encodes full-length prefusion stabilized S glycoprotein. Results from Phase III clinical trials and mass vaccination studies show promising results with high efficacy against severe COVID-19 and similar data across subgroups defined by age, sex, race, and the presence of coexisting conditions (Dagan et al., 2021; Polack et al., 2020). BNT162b2 elicited robust anti-S IgG responses and SARS-CoV-2 neutralizing titers in the trials (Walsh et al., 2020). The emergence and global spread of SARS-CoV-2 variants of concern with mutations in

the S gene first detected in the United Kingdom (B.1.1.7 lineage), South Africa (B.1.351 lineage), and Brazil (P.1 lineage), threaten to decrease the efficacy of vaccines based on the original Wuhan-Hu-1 SARS-CoV-2 S antigen. All three variants have a N501Y amino acid change in RBD, while the B.1.351 and P.1 variants both have two additional RBD changes, K417N/T and E484K, increasing the binding affinity of RBD to ACE2 (Ramanathan et al., 2021). These amino acid changes, particularly E484K, alter important epitopes targeted by many antibodies that neutralize SARS-CoV-2 by preventing RBD binding to host ACE2 (Greaney et al., 2021).

Here, we compare the longitudinal antibody responses in 55 BNT162b2 vaccine recipients and 100 COVID-19 patients, and identify key differences in the magnitude, isotype profiles, SARS-CoV-2 S domain specificity and breadth of responses targeting other human coronaviruses (HCoVs). In contrast, evaluating IgG and RBD-ACE2 blocking antibody responses to the early Wuhan-Hu-1 S protein and the three most concerning novel viral variants B.1.1.7, P.1 and B.1.351, we find remarkably consistent vulnerabilities among different individuals regardless of whether their antibody responses were stimulated by infection or vaccination.

Results

BNT162b2 vaccination induces high anti-SARS-CoV-2 IgG concentrations

We measured anti-SARS-CoV-2 antibody isotype concentrations for nucleocapsid (N), full S and S domains S1 N-terminal domain (NTD) and RBD in BNT162b2 study participant plasma samples collected before or immediately after their first dose (day 0), and on days 7, 21 (prior to the 2nd dose), 28, and 42 after the prime using multiplexed electrochemiluminescence (ECL) assays (Meso

Scale Discovery, MSD). Four of the vaccine recipients had a history of positive SARS-CoV-2 RT-qPCR tests (CoV-2+ vaccinees), while the remaining 51 participants were naïve to SARS-CoV-2 (CoV-2– vaccinees). IgG titers for S protein and its domains in CoV-2– vaccinees were negative at baseline and day 7 after their first vaccination, increased by day 21, and reached their highest levels at days 28 and 42 (Figures 1A and 1B). IgG to N protein in CoV-2– participants remained negative throughout the vaccine course as expected. The kinetics of the S protein IgG response tended to be faster for patients previously infected with SARS-CoV-2. Three of the four CoV-2+ vaccinees showed elevations in IgG antibody responses to NTD, RBD, and S by day 7 and reached higher levels than observed for the CoV-2– vaccinees at day 21. One CoV-2+ vaccinee showed slower kinetics of IgG increase, more similar to CoV-2– vaccinees (Figures 1A and 1B). CoV-2+ participant median anti-N protein IgG concentrations were increased at baseline and did not increase with vaccination.

All but two study participants had developed robust IgG responses to SARS-CoV-2 RBD and S by day 28 (Figure 1A), with CoV-2+ and CoV-2– vaccinees reaching comparable IgG concentrations (Figures 1A and 1B). One individual with low anti-RBD and anti-S responses did not receive the second vaccine dose; the other was a 70-year-old individual with a prior history of oral cancer. Two vaccinees taking methotrexate immunosuppressive medication showed no decrease in antibody responses to vaccination. All BNT162b2 recipients had weaker IgM and IgA antibody responses to S domains and full S, in comparison to their IgG responses (Figure 1A; Figures S1A and S1B).

Study participants in all age groups (< 40 years, 40 to 60 years, > 60 years) developed robust IgG antibody responses, although younger individuals reached higher Ig antibody concentrations compared to the individuals over 60 years of age (Figures 1A and 1B; Figures S1A and S1B). We

compared IgG antibody responses in vaccinees who did or did not report side effects from their prime and boost vaccination. The most common side effects reported were site tenderness, muscle aches, headaches, and fatigue (Figure S2A). None of the side effects experienced after the prime or boost vaccination were associated with an increase or decrease in IgG antibody responses (Figure S2B).

BNT162b2 vaccination and SARS-CoV-2 infection elicit distinct Ig isotype profiles

COVID-19 patients with severe disease develop higher SARS-CoV-2-specific antibody titers than asymptomatic or mildly ill individuals (Long et al., 2020; Röltgen et al., 2020). We measured the magnitude and Ig isotype profiles in moderately and severely ill COVID-19 patients sampled in the initial months of the pandemic before viral variants of concern had been reported, and compared these to the responses of BNT162b2 vaccinees, using the MSD ECL platform (Figure 2; Figure S3).

COVID-19 plasma samples were from a previously described cohort of patients who presented to Stanford Healthcare clinical sites for care (Röltgen et al., 2020). Patients were classified as outpatients; admitted patients not requiring care in the intensive care unit (ICU); ICU patients; and those who died from their illness. Serological responses measured by ECL in 530 longitudinal plasma samples from these 100 COVID-19 patients were highly correlated with results from laboratory-developed anti-RBD, -S1, and -N ELISAs (Figure S4) (Röltgen et al., 2020).

Vaccinees developed IgG antibody concentrations to the SARS-CoV-2 NTD, RBD, and S proteins that were comparable to the responses in severely ill patients, and higher than those of mildly or

moderately ill patients; this reached statistical significance for anti-NTD antibodies at days 28 and 42 and for anti-RBD antibodies at day 42. In comparison to infection, the BNT162b2 vaccine induced a highly IgG-polarized serological response, with minimal IgM and IgA responses to S and S domains RBD and NTD (Figure 2; Figure S3).

BNT162b2 vaccination produces less broad serological responses to endemic HCoVs than SARS-CoV-2 infection

While SARS-CoV-2 proteins show sequence divergence from those of other HCoVs, regions of high conservation exist at the epitope level (Ladner et al., 2021) that can lead to plasma antibody cross-reactivity. SARS-CoV-2 and SARS-CoV S proteins share 76% amino acid similarity. Serological analysis cannot readily distinguish between antibodies produced after reactivation of pre-existing HCoV antigen-specific memory B cells by SARS-CoV-2 antigens, or stimulation of novel cross-reactive antibody species by SARS-CoV-2 vaccination or infection.

In SARS-CoV-2 vaccinees and COVID-19 patients within the first weeks after vaccination or infection, respectively, antibody responses to SARS-CoV S increased. Vaccinees and severely ill patients developed similar concentrations of anti-SARS-CoV S IgG, whereas those of moderately ill patients were significantly lower. Severely ill patients had higher stimulation of SARS-CoV anti-S IgA concentrations than vaccinees and other patients (Figures 3A and 3B; Figure S5). Infection stimulated notably higher IgG responses to betacoronaviruses HCoV-OC43 and HCoV-HKU1 compared to vaccination, despite the similar magnitude of total anti-SARS-CoV-2-specific antibody responses in vaccinees and severely ill patients (Figure 2B). IgA and IgM showed similar patterns of higher responses to endemic HCoVs in severely ill patients compared to vaccinees.

HCoV responses stimulated by infection varied by isotype; notably, an IgA response to alphacoronavirus HCoV-NL63 S was seen consistently in the patient groups but was not present in vaccinated individuals.

Circulating SARS-CoV-2 variants show consistent degrees of escape from polyclonal antibody responses of vaccinees and infected patients

SARS-CoV-2 variants associated with rapidly increasing case numbers have recently emerged and spread globally. Neutralizing capability of many potent anti-SARS-CoV-2 monoclonal antibodies (mAbs) against B.1.351 is reduced or abolished, and escape from recognition by vaccinee and patient plasma has been reported (Zhou et al., 2021). We analyzed and compared variant B.1.351, P.1, and B.1.1.7 S binding and S-ACE2 blocking activity of antibodies in longitudinal plasma samples from the BNT162b2 vaccinees and COVID-19 patients. Compared with Wuhan-Hu-1, antibody binding to viral variant S and RBD antigens was reduced to similar degrees in vaccinees (Figures 4A and 4B) and patients (Figure 4C), with more marked decreases for P.1 and B.1.351. Most vaccinees developed high percentages of Wuhan-Hu-1 S-ACE2 blocking activity, peaking at day 28 (7 days post-boost). A strikingly consistent hierarchy of reduction in plasma antibody binding by variant S and RBD antigens was observed among study participants, with progressively decreased binding for B.1.1.7, P.1 and B.1.351 compared to Wuhan-Hu-1 antigens. The S-ACE2 blocking antibody assay showed highly similar reductions in blocking for B.1.351 and P.1, indicating no significant difference between the effects of the K417N versus K417T RBD changes, respectively, on ACE2 blocking antibodies (Figure 4B). Two vaccinees had low RBD and S binding and S-ACE2 blocking activity for all SARS-CoV-2 variants, including Wuhan-Hu-1.

Together, these data indicate that the effects of viral variants are remarkably consistent with an escape from polyclonal antibody responses elicited either by infection or BNT162b2 vaccination.

Discussion

One of the positive developments amid the global calamity of the SARS-CoV-2 pandemic has been the rapid design, production and deployment of remarkably effective vaccines based on lipid nanoparticle delivery of mRNA encoding the viral S antigen (Baden et al., 2021; Polack et al., 2020). Although correlates of vaccine-mediated protection are still under active study, clinical correlates and passive antibody transfer experiments in rhesus macaques support a central role for neutralizing antibodies that block the viral S protein's interaction with the host ACE2 receptor. Such antibodies are elicited by infection as well as vaccination (Chandrashekar et al., 2020; Sahin et al., 2020; Yu et al., 2020), but the shared and divergent features of the serological responses produced in response to SARS-CoV-2 antigens in these different contexts are poorly understood.

We find that BNT162b2 vaccination produces robust IgG responses to S protein, and RBD and NTD domains that are as high as those generated in the most severely ill COVID-19 patients and follow a similar time course. Side-effects following vaccination were not associated with the magnitude of the serological response. Unlike infection, which stimulates robust but short-lived IgM and IgA responses, vaccination shows a pronounced bias for IgG production. These responses were similar across the adult age range in our study but showed slightly lower levels in individuals over 60 years of age. Candidate explanations for the relative absence of IgM and IgA responses to the vaccine are the potent effect of the lipid components of the vaccine formulation in driving early and extensive IgG class-switching, potentially as a result of the reported Th1-polarized $CD4^+$ T

cell responses and vigorous germinal center formation stimulated by these vaccine components (Lederer et al., 2020; Lindgren et al., 2017; Pardi et al., 2018b). Vaccinees in our study showed higher concentrations of IgG, and similar concentrations of IgA in comparison to patients with mild COVID-19 illness. In the UK-based SIREN (SARS-CoV-2 Immunity & Reinfection Evaluation) observational cohort of health care workers, estimates of SARS-CoV-2 reinfection rates compared to primary infection rates, indicated an approximately 83% reduced risk (Hall et al., 2021). The reported 95% efficacy of BNT162b2 in preventing primary infection compares favorably with this estimate and may indicate additional protection provided by the higher IgG levels produced by the vaccine.

Compared to infection, the BNT162b2 vaccine also stimulates a less broad antibody response to endemic HCoVs, despite having anti-SARS-CoV-2 and anti-SARS-CoV IgG concentrations as high as those of the most severely ill COVID-19 patients. The four endemic coronaviruses, HCoV-OC43 and HCoV-HKU1 (*Betacoronavirus*), and HCoV-NL63 and HCoV-229E (*Alphacoronavirus*) are genetically and structurally dissimilar to SARS-CoV-2, but there are regions of conservation in the S antigen (Ladner et al., 2021). Exposure to SARS-CoV-2 antigens via vaccination or infection could potentially stimulate pre-existing cross-reactive memory B cells previously generated during infections by endemic HCoVs or could generate new primary antibody responses containing cross-reactive antibodies that recognize HCoV antigens. Recent data indicate that titers of endemic HCoV-specific antibodies do not differ between SARS-CoV-2 uninfected individuals and those who become infected with SARS-CoV-2, arguing against a protective role of cross-reactive antibodies (Anderson et al., 2021). We hypothesize that differences in the inflammatory environments during SARS-CoV-2 infection compared to vaccination, and potentially the anatomical sites where the viral antigens are encountered in

224 infection versus vaccination, may favor the more narrow SARS-CoV-2 specific antibody
225 responses seen during BNT162b2 vaccination. Infection with SARS-CoV-2 also stimulates a
226 broader repertoire of T cells specific for peptides from viral proteins beyond the S antigen, drawn
227 from both memory responses to prior endemic HCoV infection and new responses to SARS-CoV-
228 2, and therefore could provide more T cell help to a wider range of B cells in the response.

229 The recent emergence of SARS-CoV-2 variants with altered S protein and RBD sequences
230 associated with immune escape has raised concern about reduced vaccine-induced immune
231 protection. Variant B.1.1.7, first detected in September 2020 in the UK, is reported to give a 20%
232 reduction of antibody titers in serum samples from vaccinees (Muik et al., 2021), but the ChAdOx1
233 vaccine based on Wuhan-Hu-1-like S antigen showed similar efficacy for earlier circulating
234 viruses and the B.1.1.7 variant (Emary et al., 2021). Variants P.1 and B.1.351, carrying the E484K
235 and K417 amino acid changes in RBD, further decrease recognition of antibodies stimulated by
236 Wuhan-Hu-1-like S sequences, as exemplified by the poor efficacy of the ChAdOx1 vaccine
237 against B.1.351 in preventing mild-to-moderate disease (Madhi et al., 2021). Here, we find that
238 the plasmas of individuals who received prime/boost BNT162b2 vaccination, as well as COVID-
239 19 patients, show a consistent pattern of progressively decreasing binding to the S and RBD
240 antigens of B.1.1.7, P.1 and B.1.351, in that order. ACE2-blocking antibody activities were
241 significantly reduced for the P.1 and B.1.351 variant in both vaccinees and COVID-19 patients
242 collected early in the pandemic, before the spread of viral variants. These data indicate both that
243 the proportions of polyclonal plasma antibodies targeting the epitopes affected by these viral
244 variants are surprisingly consistent between different individuals and are comparable between
245 infection and vaccination. The findings further suggest that susceptibility to infection by viral
246 variants, particularly the B.1.351 and P.1 variants, is likely to be widely shared in vaccinated

247 populations, particularly as antibody titers decrease over time. Because correlates of
248 immunological protection are still under study, determining the extent of vulnerability to infection
249 will require additional correlation with epidemiological surveillance for infection of vaccinated
250 individuals over time.

251 Taken together, these results underscore the potent and highly targeted serological responses
252 stimulated by the BNT162b2 mRNA vaccine, and important differences between antibody
253 responses produced from vaccination versus infection. As investigations continue into the potential
254 role of infection-stimulated antibodies in the lingering symptoms experienced by individuals with
255 'long COVID' syndrome, it will be important to include further evaluation of the differences in
256 vaccination and infection serological responses. Other key questions that will require answers in
257 the months and years ahead include the duration of effective vaccine-stimulated serological
258 responses, and the safety and efficacy of variant-targeting vaccine boosters in previously
259 vaccinated or infected individuals. The effectiveness of the new mRNA vaccine technologies
260 seems likely to bring advances in the responses to other viral pathogens.

261

262 **Acknowledgments**

263 We acknowledge Lilit Grigoryan, Yupeng Feng, and Florian Wimmers for their help in sample
264 processing. We thank the research participants in these studies.

265 Funding: This work was supported by NIH/NIAID R01AI127877 (S.D.B.), NIH/NIAID
266 R01AI130398 (S.D.B.), NIH 1U54CA260517 (S.D.B.), NIH/NIAID HHSN272201700013C
267 (G.B.S.), an endowment to S.D.B. from the Crown Family Foundation and an Early

Postdoc.Mobility Fellowship Stipend to O.F.W. from the Swiss National Science Foundation (SNSF).

Author Contributions

K.R., S.C.A.N., M.M.D, B.P., K.C.N., S.D.B. conceptualized and designed the study. K.R., S.C.A.N. performed the experiments. P.S.A., F.Y., R.A.H., O.F.W., A.S.L., F.G., V.M., C.L., E.H., M.S., collected and processed samples. J.L.W., J.N.W., B.A.P., G.B.S. provided reagents and samples. K.R., S.C.A.N. analyzed the data and performed statistical analyses. K.R., S.C.A.N, S.D.B. wrote the manuscript. All authors provided intellectual contributions, edited and approved the manuscript.

Declaration of Interests

S.D.B. has consulted for Regeneron, Sanofi, and Novartis on topics unrelated to this study, and owns stock in AbCellera Biologics. K.C.N. reports grants from National Institute of Allergy and Infectious Diseases (NIAID), Food Allergy Research & Education (FARE), End Allergies Together (EAT); National Heart, Lung, and Blood Institute (NHLBI), and National Institute of Environmental Health Sciences (NIEHS). K.C.N. is Director of FARE and World Allergy Organization (WAO) Center of Excellence at Stanford; Advisor at Cour Pharmaceuticals; Cofounder of Before Brands, Alladapt, Latitude, and IgGenix; National Scientific Committee member for the Immune Tolerance Network (ITN) of NIAID; recipient of a Research Sponsorship

288 from Nestle; Consultant and Advisory Board Member at Before Brands, Alladapt, IgGenix,

289 NHLBI, and ProBio; and Data and Safety Monitoring Board member at NHLBI.

Figures and Figure Legends

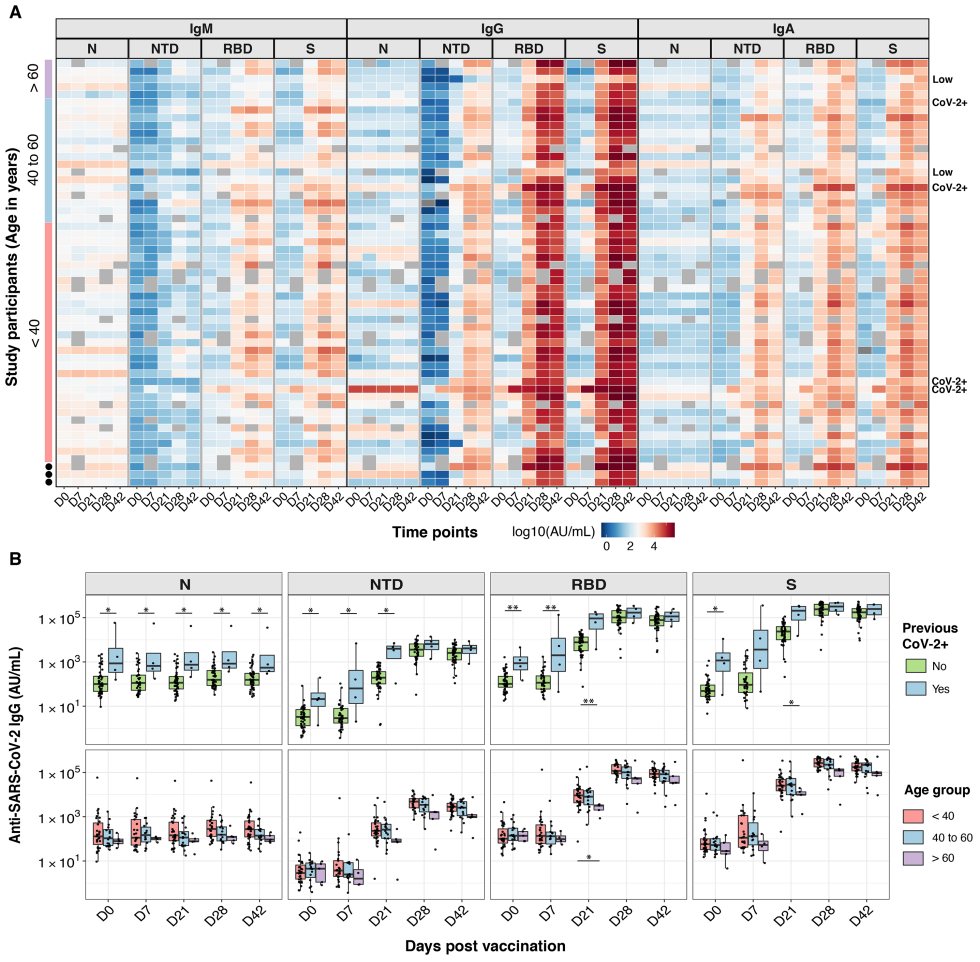

Figure 1. BNT162b2 vaccination induces high anti-SARS-CoV-2 IgG concentrations. Anti-SARS-CoV-2 N, NTD, RBD, and S IgM, IgG, and IgA antibody responses are shown for 257 plasma samples from 55 individuals who received BNT162b2 prime (day 0) and boost (day 21) vaccination doses. (A) Heatmap showing the development of antibody responses in longitudinal samples collected at day 0, 7, 21, 28, and 42 post-prime vaccination (x-axis). Log10 MSD arbitrary unit (AU)/mL concentrations are displayed for study participants sorted by age (y-axis, color-coded). Rows are labeled on the right with "CoV-2+" for participants with a previous SARS-CoV-2 RT-qPCR positive test result and with a "Low" for participants with low antibody concentrations at day 28 and day 42 post-prime. (B) Box-whisker plots of the MSD AU/mL anti-SARS-CoV-2 IgG concentrations show the interquartile range as the box and the minimum and maximum values as the ends of the whiskers. Comparisons between two groups (CoV-2+ and CoV-2) were by the two-sided Wilcoxon rank sum test; comparison between age groups (< 40; 40 to 60; > 60 years) was tested using pairwise Wilcoxon rank sum test with Bonferroni correction. * = $P < 0.05$, ** = $P < 0.01$, *** = $P < 0.001$.

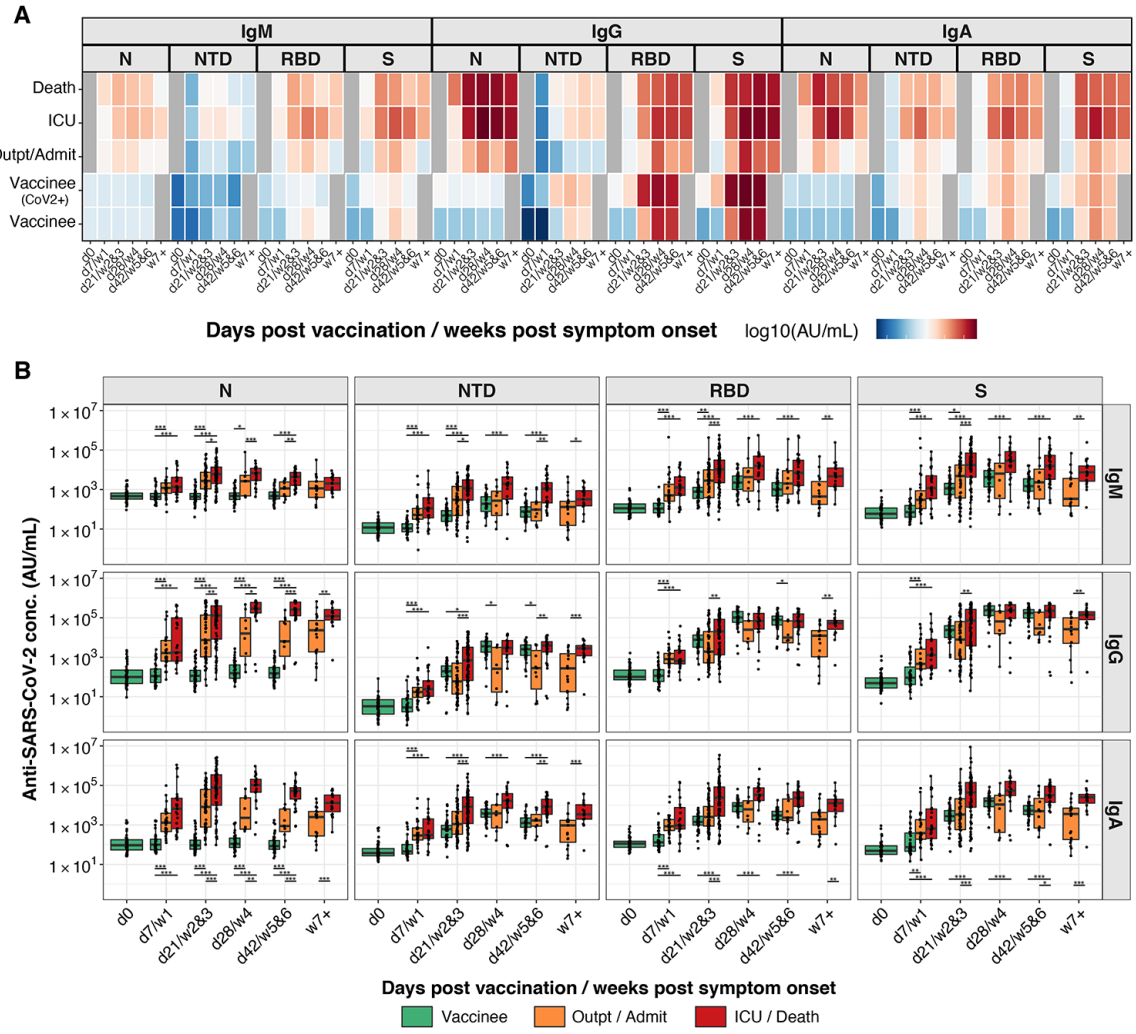

Figure 2. BNT162b2 vaccination and SARS-CoV-2 infection elicit distinct Ig isotype profiles. Anti-SARS-CoV-2 N, NTD, RBD, and S IgM, IgG, and IgA antibody responses are shown for individuals who received BNT162b2 prime (day 0) and boost (day 21) vaccination doses and for COVID-19 patients. (A) Heatmap showing the development of antibody responses in longitudinal samples from vaccinees/patients collected at / during day 0, day 7 / week 1, day 21 / weeks 2&3, day 28 / week 4, day 42 / weeks 5&6, and week 7 and later after vaccination / COVID-19 symptom onset (x-axis). Individuals were classified as outpatients (Outpt) and hospital admitted patients (Admit); intensive care unit (ICU) patients, those who died from their illness (Death) and vaccinees who did (CoV-2+) or did not have a positive SARS-CoV-2 test in the past. The color scale encodes the median values of log10 MSD arbitrary unit (AU)/mL concentrations. (B) Box-whisker plots of the MSD AU/mL anti-SARS-CoV-2 Ig concentrations show the interquartile range as the box and the minimum and maximum values as the ends of the whiskers. Statistical test for significance between groups (Outpatient/Admit; ICU/Death; Vaccinees) was performed using pairwise Wilcoxon rank sum test with Bonferroni correction. * = $P < 0.05$, ** = $P < 0.01$, *** = $P < 0.001$.

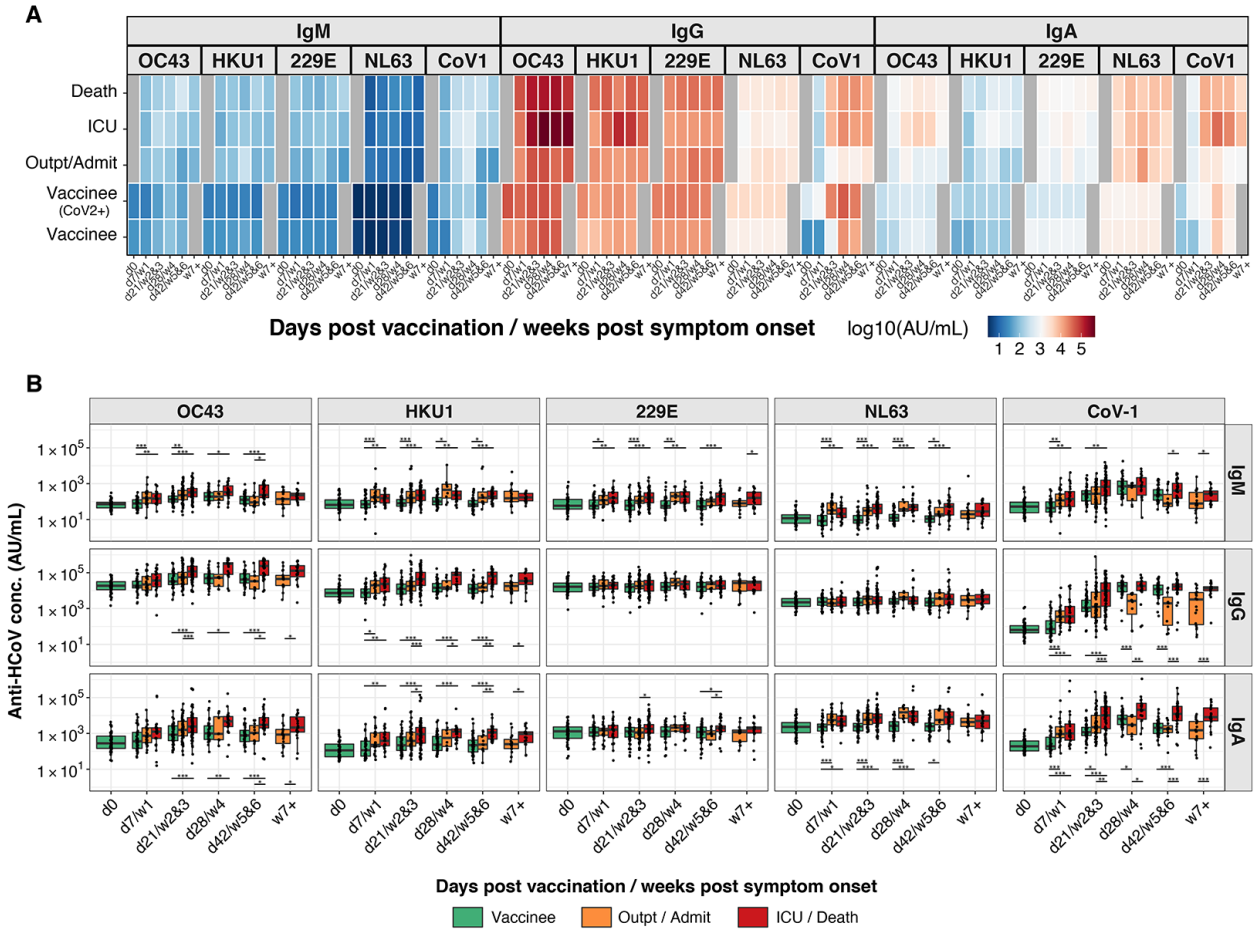

321

322 **Figure 3. BNT162b2 vaccination produces less broad serological responses to endemic**
323 **HCoVs than SARS-CoV-2 infection.** Anti-SARS-CoV S, and anti-HCoV-OC43, -HKU1, -NL63
324 and -229E S IgM, IgG, and IgA antibody responses are shown for individuals who received
325 BNT162b2 prime (day 0) and boost (day 21) vaccination doses and for COVID-19 patients. (A)
326 Heatmap showing the development of antibody responses in longitudinal samples from
327 vaccinees/patients collected at / during day 0, day 7 / week 1, day 21 / weeks 2&3, day 28 / week
328 4, day 42 / weeks 5&6, and week 7 and later after vaccination / COVID-19 symptom onset (x-
329 axis). Individuals were classified as outpatients (Outpt) and hospital admitted patients (Admit);
330 intensive care unit (ICU) patients, those who died from their illness (Death) and vaccinees who
331 did (CoV-2+) or did not have a positive SARS-CoV-2 test in the past. The color scale encodes the
332 median values of log10 MSD arbitrary unit (AU)/mL concentrations. (B) Box-whisker plots of the
333 MSD AU/mL anti-SARS-CoV-2 Ig concentrations show the interquartile range as the box and the
334 minimum and maximum values as the ends of the whiskers. Statistical test: pairwise Wilcoxon
335 rank sum test with Bonferroni correction. * = $P < 0.05$, ** = $P < 0.01$, *** = $P < 0.001$.

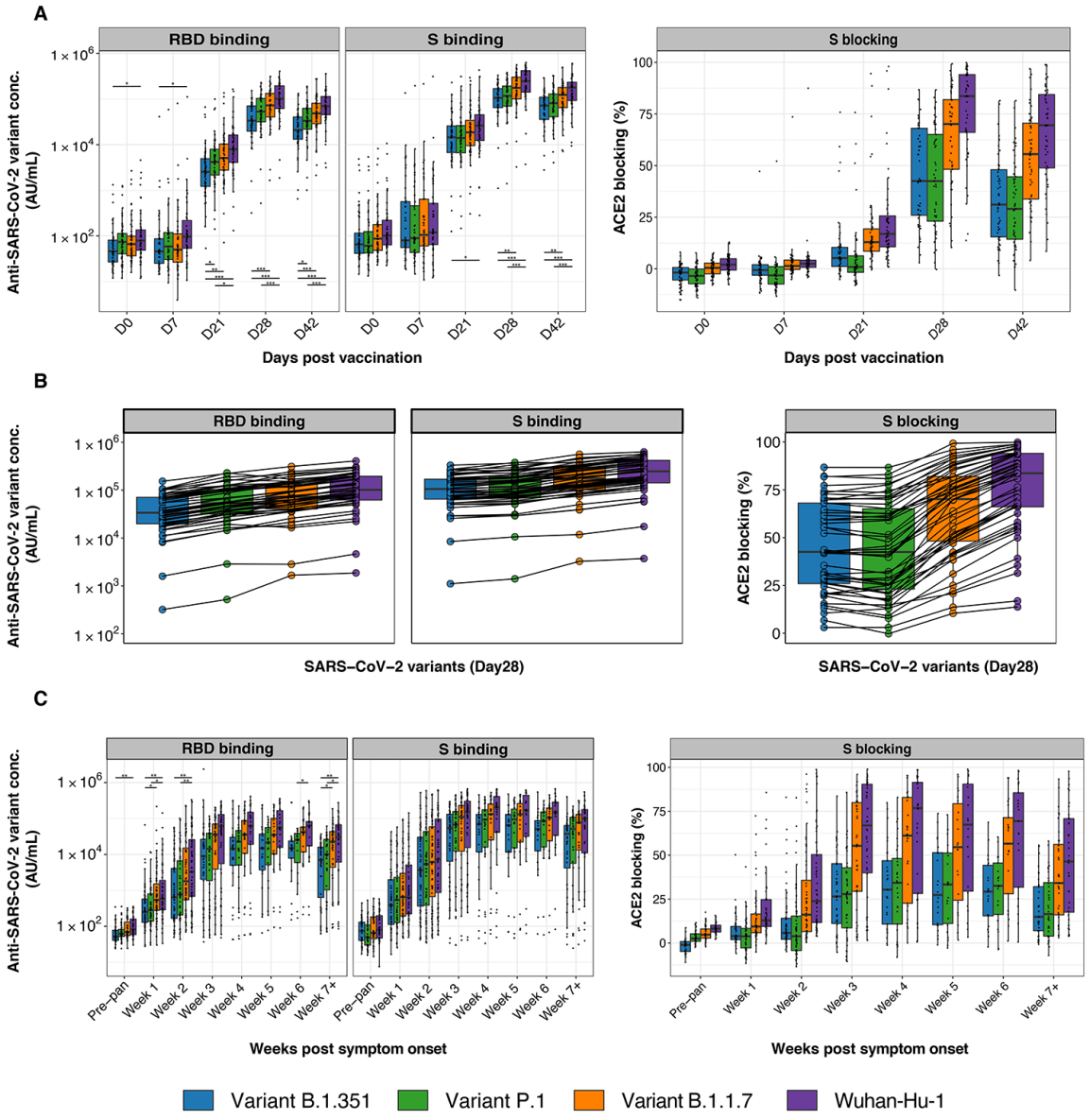

Figure 4. Circulating SARS-CoV-2 variants show consistent degrees of escape from polyclonal antibody responses of vaccinees and infected patients. Anti-SARS-CoV-2 RBD and S antibody responses are shown for Wuhan-Hu-1 and viral variants of concern (B.1.1.7, UK; P.1, Brazil; B.1.351, South Africa). Box-whisker plots of the MSD AU/mL anti-SARS-CoV-2 IgG binding concentrations and S-ACE2 blocking percentages show the interquartile range as the box and the minimum and maximum values as the ends of the whiskers. (A) Plasma samples from BNT162b2 vaccinees. (B) Comparison of antibody concentrations of BNT162b2 vaccinees on day 28 for different variants of concern. Data points for individual study participants are connected with a line. (C) Plasma samples from COVID-19 patients. Significance between groups (Wuhan-Hu-1, B.1.1.7, P.1, and B.1.351) was tested with pairwise Wilcoxon rank sum test with Bonferroni correction. * = $P < 0.05$, ** = $P < 0.01$, *** = $P < 0.001$.

Supplemental Figures

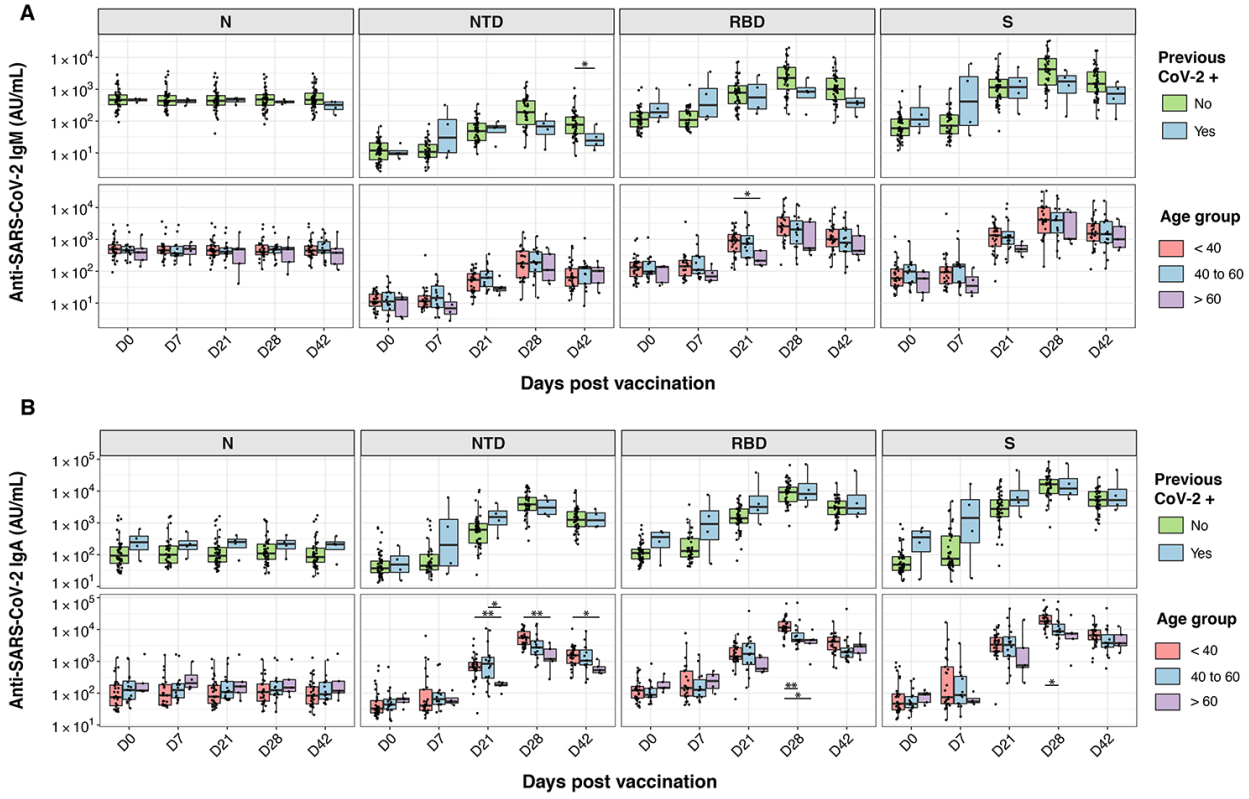

Figure S1: BNT162b2 vaccination induces variable and relatively low anti-SARS-CoV-2 IgM and IgA concentrations. Anti-SARS-CoV-2 N, NTD, RBD, and S IgM (A) and IgA (B) antibody responses are shown for 257 plasma samples from 55 individuals who received BNT162b2 prime (day 0) and boost (day 21) vaccination doses. Box-whisker plots of the MSD AU/mL anti-SARS-CoV-2 IgG concentrations show the interquartile range as the box and the minimum and maximum values as the ends of the whiskers. Statistical tests: two-sided Wilcoxon rank sum test (A and B, top panels) and pairwise Wilcoxon rank sum test with Bonferroni correction (A and B, bottom panels). * = $P < 0.05$, ** = $P < 0.01$, *** = $P < 0.001$.

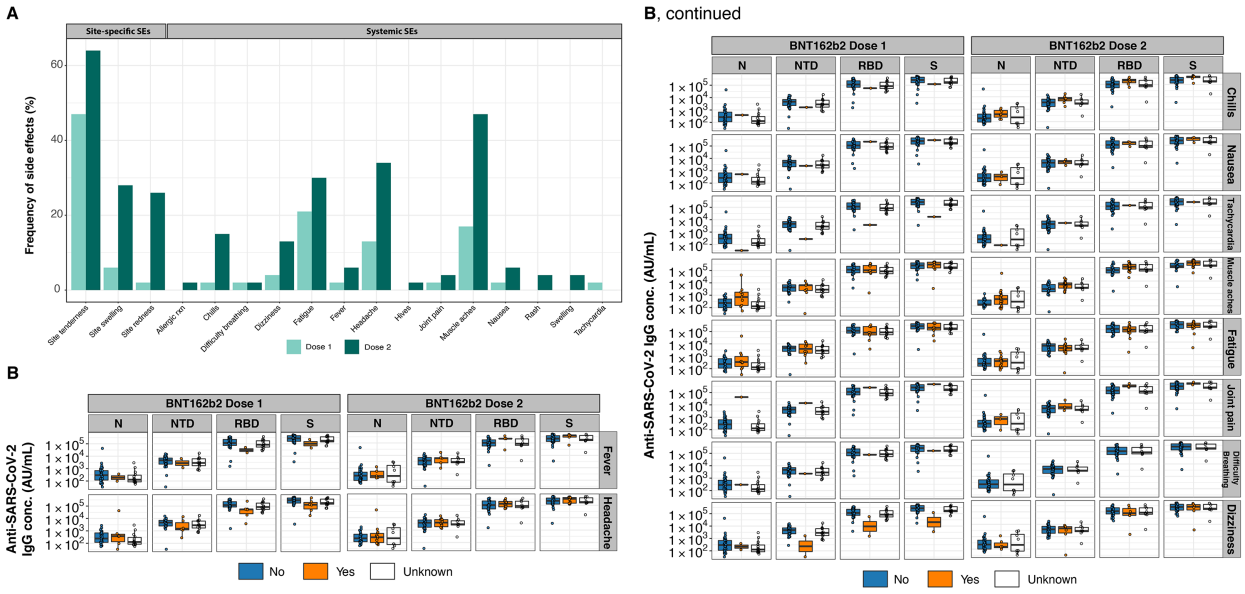

Figure S2: The magnitude of antibody responses is not correlated with reported vaccine-associated side effects (SEs). (A) Frequency of vaccine-associated side effects after the prime (light green) and boost (dark green) vaccination dose. (B) Box-whisker plots of the MSD AU/mL anti-SARS-CoV-2 IgG concentrations show the interquartile range as the box and the minimum and maximum values as the ends of the whiskers. For a given SE (horizontal panels), vaccinees were grouped according to no SE reported ("No", colored in blue) or SE reported ("Yes", colored in orange). Vaccinees where SEs were unknown are shown as white boxplots.

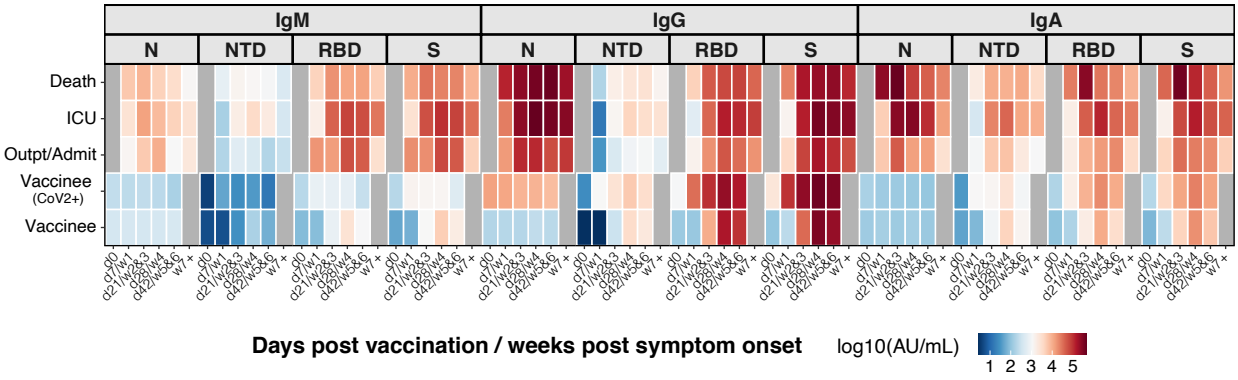

368

369 **Figure S3: BNT162b2 vaccination and SARS-CoV-2 infection elicit divergent Ig isotype**
370 **profiles.** Anti-SARS-CoV-2 N, NTD, RBD, and S IgM, IgG, and IgA antibody responses are
371 shown for individuals who received BNT162b2 prime (day 0) and boost (day 21) vaccination doses
372 and for COVID-19 patients. The heatmap shows the development of antibody responses in
373 longitudinal samples from vaccinees/patients collected at / during day 0, day 7 / week 1, day 21 /
374 weeks 2&3, day 28 / week 4, day 42 / weeks 5&6, and week 7 and later after vaccination / COVID-
375 19 symptom onset (x-axis). Individuals were classified as outpatients (Outpt) and hospital admitted
376 patients (Admit); intensive care unit (ICU) patients, those who died from their illness (Death) and
377 vaccinees who did (CoV-2+) or did not have a positive SARS-CoV-2 test in the past. **Mean** values
378 (as opposed to the **Median** values shown in the main Figure 2) of log10 MSD arbitrary unit
379 (AU)/mL concentrations were used to display a color code for each of the study groups.

380

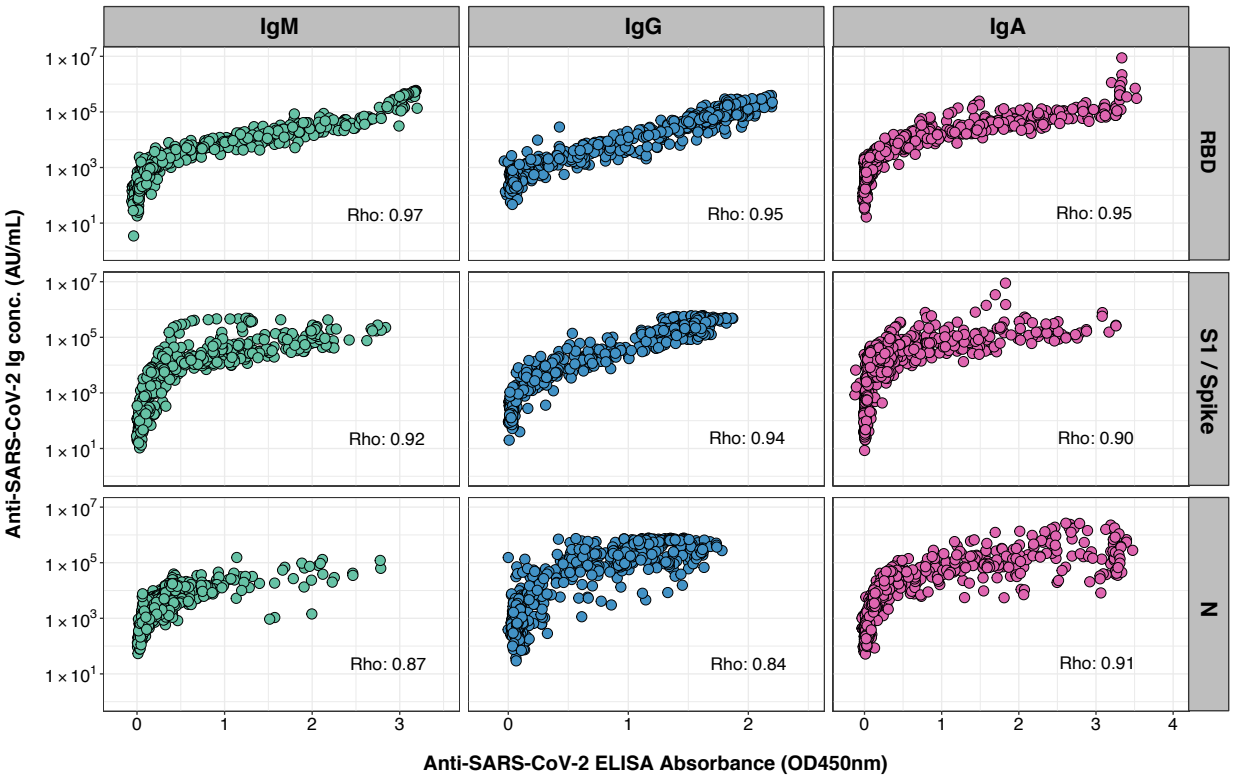

Figure S4: Correlation of anti-SARS-CoV-2 ELISA and ECL results. Anti-SARS-CoV-2 RBD, S1/S, and N IgM, IgG, and IgA antibody responses were measured in 530 plasma samples from 100 COVID-19 patients by ELISA and MSD ECL assays. ELISA versus MSD RBD and N assay results and ELISA S1 versus MSD S assay results were highly correlated. Spearman rank correlation (coefficient = Rho, displayed in the plot for each assay comparison) was used to assess the strength of correlation between ELISA and MSD results. Outliers for the N assays with less correlated ELISA and MSD results may be attributed to the fact that the N protein used in the ELISAs was produced in *E. coli*, whereas the MSD N protein was produced in mammalian cells, potentially causing differences in post-translational modifications and thus epitope recognition.

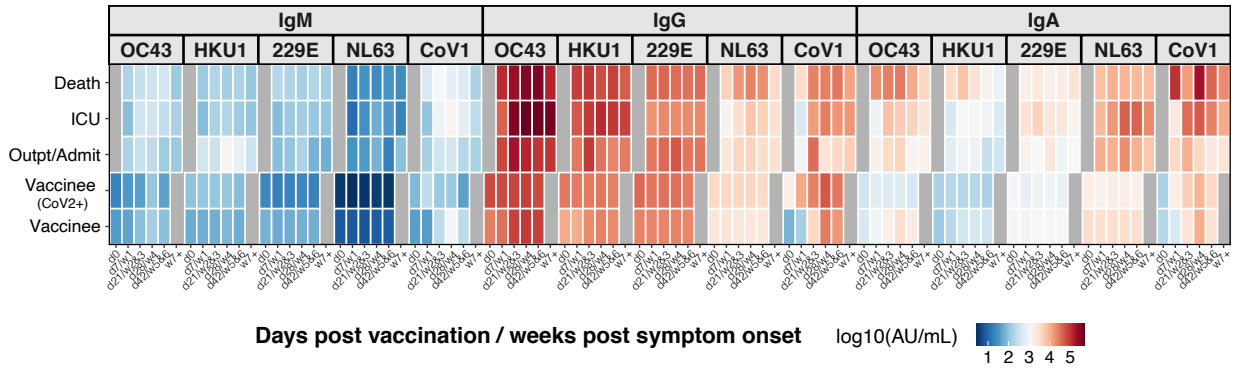

392

393 **Figure S5: Less broad serological responses to endemic HCoVs from BNT162b2 compared**
394 **to SARS-CoV-2 infection.** Anti-SARS-CoV S, and anti-HCoV-OC43, -HKU1, -NL63 and -229E
395 S IgM, IgG, and IgA antibody responses are shown for individuals who received BNT162b2 prime
396 (day 0) and boost (day 21) vaccination doses and for COVID-19 patients. The heatmap shows the
397 development of antibody responses in longitudinal samples from vaccinees/patients collected at /
398 during day 0, day 7 / week 1, day 21 / weeks 2&3, day 28 / week 4, day 42 / weeks 5&6, and week
399 7 and later after vaccination / COVID-19 symptom onset (x-axis). Individuals were classified as
400 outpatients (Outpt) and hospital admitted patients (Admit); intensive care unit (ICU) patients, those
401 who died from their illness (Death) and vaccinees who did (CoV-2+) or did not have a positive
402 SARS-CoV-2 test in the past. **Mean** values (as opposed to the **Median** values shown in the main
403 Figure 3) of log10 MSD arbitrary unit (AU)/mL concentrations were used to display a color code
404 for each of the study groups.

Tables

Table 1. Demographic characteristics of vaccine study participants.

Characteristics		BNT162b2 vaccinees (n = 55)
Demographic information available, n (%)		52 (95)
Age, median (IQR)		36 (31.5 – 50)
Sex, n (%)	**Female**	27 (49)
	Male	25 (45)
Race*, n (%)	**Asian**	22 (40)
	Black	3 (5)
	White	24 (44)
Previous SARS-CoV-2+ test result, n (%)		4 (7)

* two individuals reported to be American and one individual reported to be Indian and were thus not assigned to either of the groups.

STAR Methods

RESOURCE AVAILABILITY

Lead Contact

Further information and requests for resources and reagents should be directed to the Lead Contact, Scott D. Boyd (sboyd1@stanford.edu).

Data and Code Availability

All data is available in the main text or the extended materials. Code will be provided to readers upon request.

EXPERIMENTAL MODELS AND SUBJECT DETAILS

Samples from BNT162b2 vaccinees

All participants in the study provided informed consent, under Stanford University Institutional Review Board approved protocol IRB-55689. To study immune responses after first and second dose vaccination with BNT162b2, we included 257 longitudinal samples from 55 vaccinees. Samples were collected on day 0 before or immediately after the first vaccination dose and individuals received their second dose on day 21. Time points in the manuscript are defined as day 7, 21, 28, and 42 and blood was drawn +/- one day from the assigned time point. Peripheral blood samples were collected in vacutainer cell preparation tubes (CPT) containing sodium citrate. After

centrifugation for collection of plasma, samples were aliquoted and stored at -80°C. Demographic information for all vaccinees is provided in Table 1.

Samples from COVID-19 patients

We included 530 plasma samples collected between March 2020 and August 2020 from patients who reported to Stanford Healthcare-associated clinical sites with signs and symptoms of COVID-19. SARS-CoV-2 infection was confirmed for all patients by reverse-transcription quantitative polymerase chain reaction (RT-qPCR) of nasopharyngeal swabs as described (Corman et al., 2020; Hogan et al., 2020). Data for SARS-CoV-2 serology measurements on these samples by ELISA have been reported previously (Röltgen et al., 2020). Blood samples were collected in sodium heparin-coated vacutainers. After centrifugation for collection of plasma, samples were aliquoted and stored at -80°C. The use of these samples for serology testing was approved by the Stanford University Institutional Review Board (Protocols IRB-48973 and IRB-55689).

Healthy human control (HHC) samples

37 plasma samples from HHCs collected before the onset of the COVID-19 pandemic were used to determine baseline antibody binding to coronavirus antigens.

METHOD DETAILS

MSD ECL binding assays

Plasma samples from vaccinees and COVID-19 patients were heat-inactivated at 56°C for 30 minutes and tested with MSD ECL MULTI-SPOT 96-well plate serology panels and instrumentation according to the manufacturer's instructions. V-PLEX Coronavirus Panel 2 kits were used to detect IgM, IgG, and IgA antibodies to SARS-CoV-2 N, S1 NTD, RBD, and S antigens and to S proteins of SARS-CoV and other HCoVs including HCoV-OC43, HCoV-HKU1, HCoV-NL63, and HCoV-229E. V-PLEX SARS-CoV-2 Panel 7 kits were used to detect IgG antibodies to different SARS-CoV-2 variant RBD and S proteins, including Wuhan-Hu-1, B.1.351, P.1, and B.1.1.7. Plasma samples were analyzed in duplicate at a 1:5'000 dilution, detected with anti-human IgM, IgG, or IgA antibodies conjugated to SULFO-TAG ECL labels and read with a MESO QuickPlex SQ 120 instrument. Each plate contained duplicates of a 7-point calibration curve with serial dilution of a reference standard, a blank well and three positive control samples. Calibration curves were used to calculate antibody unit concentrations (MSD AU/mL) by backfitting ECL signals measured for each sample to the curve.

MSD ECL blocking assays

Antibodies blocking the binding of SARS-CoV-2 RBD to ACE2 were detected with MSD V-PLEX SARS-CoV-2 Panel 7 (ACE2) kits according to the manufacturer's instructions. Heat-inactivated plasma samples from vaccinees and COVID-19 patients were analyzed in duplicate at a dilution of 1:100. Samples were incubated together with human ACE2 protein conjugated with

a SULFO-TAG and read with a MESO QuickPlex SQ 120 instrument. Each plate contained duplicates of a 7-point calibration curve with serial dilution of a reference standard and a blank well. Results are reported as percent inhibition calculated based on the equation ((1 – Average Sample ECL Signal / Average ECL signal of blank well) x 100).

ELISA testing of COVID-19 patient samples

ELISA testing of the 530 COVID-19 patient samples for the presence of antibodies to SARS-CoV-2 antigens was performed previously (Röltgen et al., 2020). To compare the performance of the MSD SARS-CoV-2 panel plates with our laboratory developed ELISAs we included results for anti-SARS-CoV-2 RBD, S1, and N IgM, IgG, and IgA ELISA testing in this study. Briefly, ELISA was performed after coating 96-well Corning Costar high binding plates (catalog no. 9018, Thermo Fisher) SARS-CoV-2 RBD, S1, or N protein in phosphate-buffered saline (PBS) at a concentration of 0.1 μg per well (0.025 μg per well for the nucleocapsid IgG assay) overnight at 4°C. On the next day, plates were blocked, and wells were then incubated with plasma samples from COVID-19 patients at a dilution of 1:100. Bound antibodies were detected with horseradish peroxidase conjugated goat anti-human IgG (γ-chain specific, catalog no. 62-8420, Thermo Fisher, 1:6,000 dilution), IgM (μ-chain specific, catalog no. A6907, Sigma, 1:6,000 dilution), or IgA (α-chain specific, catalog no. P0216, Agilent, 1:5,000 dilution). 3,3′,5,5′-Tetramethylbenzidine (TMB) substrate solution was added and the reaction was stopped after 12 min by addition of 0.16 M sulfuric acid. The optical density (OD) at 450 nanometers was measured with an EMax Plus microplate reader (Molecular Devices, San Jose, CA).

QUANTIFICATION AND STATISTICAL ANALYSIS

Statistical tests were performed in R using base packages for statistical analysis and the ggplot2 package was used for graphics. Box-whisker plots show median (horizontal line), interquartile range (box), and 1.5 times the interquartile range (whiskers). In all analyses where statistical significance was tested, significance was defined as: ***p-value < 0.001; **p-value < 0.01; *p-value $\leq$ 0.05.

References

Anderson, E.M., Goodwin, E.C., Verma, A., Arevalo, C.P., Bolton, M.J., Weirick, M.E., Gouma, S., McAllister, C.M., Christensen, S.R., Weaver, J., et al. (2021). Seasonal human coronavirus antibodies are boosted upon SARS-CoV-2 infection but not associated with protection. Cell *184*, 1858-1864.e10.

Baden, L.R., El Sahly, H.M., Essink, B., Kotloff, K., Frey, S., Novak, R., Diemert, D., Spector, S.A., Rouphael, N., Creech, C.B., et al. (2021). Efficacy and Safety of the mRNA-1273 SARS-CoV-2 Vaccine. New England Journal of Medicine *384*, 403–416.

Chandrashekar, A., Liu, J., Martinot, A.J., McMahan, K., Mercado, N.B., Peter, L., Tostanoski, L.H., Yu, J., Maliga, Z., Nekorchuk, M., et al. (2020). SARS-CoV-2 infection protects against rechallenge in rhesus macaques. Science *369*, 812–817.

Corman, V.M., Landt, O., Kaiser, M., Molenkamp, R., Meijer, A., Chu, D.K., Bleicker, T., Brünink, S., Schneider, J., Schmidt, M.L., et al. (2020). Detection of 2019 novel coronavirus (2019-nCoV) by real-time RT-PCR. Euro Surveill. *25*.

Dagan, N., Barda, N., Kepten, E., Miron, O., Perchik, S., Katz, M.A., Hernán, M.A., Lipsitch, M., Reis, B., and Balicer, R.D. (2021). BNT162b2 mRNA Covid-19 Vaccine in a Nationwide Mass Vaccination Setting. New England Journal of Medicine *0*, null.

Emary, K.R.W., Golubchik, T., Aley, P.K., Ariani, C.V., Angus, B., Bibi, S., Blane, B., Bonsall, D., Cicconi, P., Charlton, S., et al. (2021). Efficacy of ChAdOx1 nCoV-19 (AZD1222) vaccine against SARS-CoV-2 variant of concern 202012/01 (B.1.1.7): an exploratory analysis of a randomised controlled trial. The Lancet *0*.

Greaney, A.J., Loes, A.N., Crawford, K.H.D., Starr, T.N., Malone, K.D., Chu, H.Y., and Bloom, J.D. (2021). Comprehensive mapping of mutations to the SARS-CoV-2 receptor-binding domain that affect recognition by polyclonal human serum antibodies. BioRxiv 2020.12.31.425021.

Hall, V., Foulkes, S., Charlett, A., Atti, A., Monk, E.J.M., Simmons, R., Wellington, E., Cole, M.J., Saei, A., Oguti, B., et al. (2021). Do antibody positive healthcare workers have lower SARS-CoV-2 infection rates than antibody negative healthcare workers? Large multi-centre prospective cohort study (the SIREN study), England: June to November 2020. MedRxiv 2021.01.13.21249642.

Hogan, C.A., Sahoo, M.K., Huang, C., Garamani, N., Stevens, B., Zehnder, J., and Pinsky, B.A. (2020). Comparison of the Panther Fusion and a laboratory-developed test targeting the envelope gene for detection of SARS-CoV-2. J Clin Virol *127*, 104383.

Ladner, J.T., Henson, S.N., Boyle, A.S., Engelbrektson, A.L., Fink, Z.W., Rahee, F., D'ambrozio, J., Schaecher, K.E., Stone, M., Dong, W., et al. (2021). Epitope-resolved profiling of the SARS-CoV-2 antibody response identifies cross-reactivity with endemic human coronaviruses. Cell Rep Med *2*, 100189.

538 Lederer, K., Castaño, D., Gómez Atria, D., Oguin, T.H., Wang, S., Manzoni, T.B., Muramatsu,
539 H., Hogan, M.J., Amanat, F., Cherubin, P., et al. (2020). SARS-CoV-2 mRNA Vaccines Foster
540 Potent Antigen-Specific Germinal Center Responses Associated with Neutralizing Antibody
541 Generation. Immunity *53*, 1281-1295.e5.

542 Lindgren, G., Ols, S., Liang, F., Thompson, E.A., Lin, A., Hellgren, F., Bahl, K., John, S.,
543 Yuzhakov, O., Hassett, K.J., et al. (2017). Induction of Robust B Cell Responses after Influenza
544 mRNA Vaccination Is Accompanied by Circulating Hemagglutinin-Specific ICOS+ PD-1+
545 CXCR3+ T Follicular Helper Cells. Front. Immunol. *8*.

546 Long, Q.-X., Liu, B.-Z., Deng, H.-J., Wu, G.-C., Deng, K., Chen, Y.-K., Liao, P., Qiu, J.-F., Lin,
547 Y., Cai, X.-F., et al. (2020). Antibody responses to SARS-CoV-2 in patients with COVID-19.
548 Nature Medicine 1–4.

549 Madhi, S.A., Baillie, V., Cutland, C.L., Voysey, M., Koen, A.L., Fairlie, L., Padayachee, S.D.,
550 Dheda, K., Barnabas, S.L., Bhorat, Q.E., et al. (2021). Efficacy of the ChAdOx1 nCoV-19
551 Covid-19 Vaccine against the B.1.351 Variant. New England Journal of Medicine.

552 McMahan, K., Yu, J., Mercado, N.B., Loos, C., Tostanoski, L.H., Chandrashekar, A., Liu, J.,
553 Peter, L., Atyeo, C., Zhu, A., et al. (2021). Correlates of protection against SARS-CoV-2 in
554 rhesus macaques. Nature *590*, 630–634.

555 Muik, A., Wallisch, A.-K., Sänger, B., Swanson, K.A., Mühl, J., Chen, W., Cai, H., Maurus, D.,
556 Sarkar, R., Türeci, Ö., et al. (2021). Neutralization of SARS-CoV-2 lineage B.1.1.7 pseudovirus
557 by BNT162b2 vaccine–elicited human sera. Science *371*, 1152–1153.

558 Ni, L., Ye, F., Cheng, M.-L., Feng, Y., Deng, Y.-Q., Zhao, H., Wei, P., Ge, J., Gou, M., Li, X., et
559 al. (2020). Detection of SARS-CoV-2-Specific Humoral and Cellular Immunity in COVID-19
560 Convalescent Individuals. Immunity *52*, 971-977.e3.

561 Pardi, N., Hogan, M.J., Pelc, R.S., Muramatsu, H., Andersen, H., DeMaso, C.R., Dowd, K.A.,
562 Sutherland, L.L., Scearce, R.M., Parks, R., et al. (2017). Zika virus protection by a single low-
563 dose nucleoside-modified mRNA vaccination. Nature *543*, 248–251.

564 Pardi, N., Hogan, M.J., Porter, F.W., and Weissman, D. (2018a). mRNA vaccines — a new era
565 in vaccinology. Nature Reviews Drug Discovery *17*, 261–279.

566 Pardi, N., Hogan, M.J., Naradikian, M.S., Parkhouse, K., Cain, D.W., Jones, L., Moody, M.A.,
567 Verkerke, H.P., Myles, A., Willis, E., et al. (2018b). Nucleoside-modified mRNA vaccines
568 induce potent T follicular helper and germinal center B cell responses. J Exp Med *215*, 1571–
569 1588.

570 Pardi, N., LaBranche, C.C., Ferrari, G., Cain, D.W., Tombácz, I., Parks, R.J., Muramatsu, H.,
571 Mui, B.L., Tam, Y.K., Karikó, K., et al. (2019). Characterization of HIV-1 Nucleoside-Modified
572 mRNA Vaccines in Rabbits and Rhesus Macaques. Mol Ther Nucleic Acids *15*, 36–47.

573 Polack, F.P., Thomas, S.J., Kitchin, N., Absalon, J., Gurtman, A., Lockhart, S., Perez, J.L., Pérez
574 Marc, G., Moreira, E.D., Zerbini, C., et al. (2020). Safety and Efficacy of the BNT162b2 mRNA
575 Covid-19 Vaccine. New England Journal of Medicine *383*, 2603–2615.

576 Ramanathan, M., Ferguson, I.D., Miao, W., and Khavari, P.A. (2021). SARS-CoV-2 B.1.1.7 and
577 B.1.351 Spike variants bind human ACE2 with increased affinity. BioRxiv.

578 Richner, J.M., Himansu, S., Dowd, K.A., Butler, S.L., Salazar, V., Fox, J.M., Julander, J.G.,
579 Tang, W.W., Shresta, S., Pierson, T.C., et al. (2017). Modified mRNA Vaccines Protect against
580 Zika Virus Infection. Cell *168*, 1114-1125.e10.

581 Röltgen, K., Powell, A.E., Wirz, O.F., Stevens, B.A., Hogan, C.A., Najeeb, J., Hunter, M.,
582 Wang, H., Sahoo, M.K., Huang, C., et al. (2020). Defining the features and duration of antibody
583 responses to SARS-CoV-2 infection associated with disease severity and outcome. Sci Immunol
584 *5*.

585 Rydyznski Moderbacher, C., Ramirez, S.I., Dan, J.M., Grifoni, A., Hastie, K.M., Weiskopf, D.,
586 Belanger, S., Abbott, R.K., Kim, C., Choi, J., et al. (2020). Antigen-Specific Adaptive Immunity
587 to SARS-CoV-2 in Acute COVID-19 and Associations with Age and Disease Severity. Cell *183*,
588 996-1012.e19.

589 Sahin, U., Karikó, K., and Türeci, Ö. (2014). mRNA-based therapeutics — developing a new
590 class of drugs. Nature Reviews Drug Discovery *13*, 759–780.

591 Sahin, U., Muik, A., Vogler, I., Derhovanessian, E., Kranz, L.M., Vormehr, M., Quandt, J.,
592 Bidmon, N., Ulges, A., Baum, A., et al. (2020). BNT162b2 induces SARS-CoV-2-neutralising
593 antibodies and T cells in humans. MedRxiv 2020.12.09.20245175.

594 Vogel, A.B., Kanevsky, I., Che, Y., Swanson, K.A., Muik, A., Vormehr, M., Kranz, L.M.,
595 Walzer, K.C., Hein, S., Güler, A., et al. (2021). BNT162b vaccines protect rhesus macaques
596 from SARS-CoV-2. Nature.

597 Walsh, E.E., Frenck, R.W., Falsey, A.R., Kitchin, N., Absalon, J., Gurtman, A., Lockhart, S.,
598 Neuzil, K., Mulligan, M.J., Bailey, R., et al. (2020). Safety and Immunogenicity of Two RNA-
599 Based Covid-19 Vaccine Candidates. New England Journal of Medicine *383*, 2439–2450.

600 Yu, J., Tostanoski, L.H., Peter, L., Mercado, N.B., McMahan, K., Mahrokhian, S.H., Nkolola,
601 J.P., Liu, J., Li, Z., Chandrashekar, A., et al. (2020). DNA vaccine protection against SARS-
602 CoV-2 in rhesus macaques. Science *369*, 806–811.

603 Yuan, M., Liu, H., Wu, N.C., and Wilson, I.A. (2021). Recognition of the SARS-CoV-2 receptor
604 binding domain by neutralizing antibodies. Biochemical and Biophysical Research
605 Communications *538*, 192–203.

606 Zhang, C., Maruggi, G., Shan, H., and Li, J. (2019). Advances in mRNA Vaccines for Infectious
607 Diseases. Front. Immunol. *10*.

608 Zhou, D., Dejnirattisai, W., Supasa, P., Liu, C., Mentzer, A.J., Ginn, H.M., Zhao, Y.,
609 Duyvesteyn, H.M.E., Tuekprakhon, A., Nutalai, R., et al. (2021). Evidence of escape of SARS-
610 CoV-2 variant B.1.351 from natural and vaccine-induced sera. Cell.

611